Climate forcing insufficient to explain sea-level lowstands in Maldives during Common Era

Christopher Piecuch[1,1], Andrew Kemp[2,2], Geoffrey Gebbie[1,1], and Aron Meltzner[3]

[1]Woods Hole Oceanographic Institution
[2]Tufts University
[3]Nanyang Technological University, Singapore

November 30, 2022

Abstract

Reconstructions of Common-Era sea level are informative of relationships between sea level and natural climate variation, and the uniqueness of modern sea-level rise. Kench et al. recently reconstructed Common-Era sea level in the Maldives, Indian Ocean, using coral microatolls. They reported periods of 150-500 yr when sea level fell and rose at average rates of 2.7-4.3 mm/yr. These periods coincided with intervals of cooling and warming inferred from proxy reconstructions of sea-surface temperature (SST) and radiative forcing (ref. 2, Fig. 2). Kench et al. reasoned that these 0.6-1.4-m centennial-scale sea-level fluctuations were driven by climate, specifically thermal contraction and expansion of seawater. In contrast to previous studies, Kench et al. argued that modern rates and magnitudes of sea-level rise caused by climate change have precedent during the Common Era. We use principles of sea-level physics to argue that pre-industrial radiative forcing and SST changes were insufficient to cause thermosteric sea-level (TSL) trends as large as reported for the Maldives.

Coversheet for “Climate forcing insufficient to drive apparent Common-Era sea-level lowstands in Maldives”

Christopher G. Piecuch[1,†], Andrew C. Kemp[2,‡], Geoffrey Gebbie[1,*], & Aron J. Meltzner[3,4,⊛]

[1] *Department of Physical Oceanography, Woods Hole Oceanographic Institution, Woods Hole, Massachusetts, USA*

[2] *Department of Earth and Ocean Sciences, Tufts University, Medford, Massachusetts, USA*

[3] *Earth Observatory of Singapore, Nanyang Technological University, Singapore*

[4] *Asian School of the Environment, Nanyang Technological University, Singapore*

This paper submitted to Earth and Space Science Open Archive (ESSOAr) has undergone one round of peer review and is now under revision at Nature Geoscience as a “Matters Arising.”

† cpiecuch@whoi.edu

‡ andrew.kemp@tufts.edu

∗ jgebbie@whoi.edu

⊛ meltzner@ntu.edu.sg

Climate forcing insufficient to drive apparent Common-Era sea-level lowstands in Maldives

Christopher G. Piecuch[1], Andrew C. Kemp[2], Geoffrey Gebbie[1], & Aron J. Meltzner[3,4]

[1]*Department of Physical Oceanography, Woods Hole Oceanographic Institution, Woods Hole, Massachusetts, USA*

[2]*Department of Earth and Ocean Sciences, Tufts University, Medford, Massachusetts, USA*

[3]*Earth Observatory of Singapore, Nanyang Technological University, Singapore*

[4]*Asian School of the Environment, Nanyang Technological University, Singapore*

Reconstructions of Common-Era sea level are informative of relationships between sea level and natural climate variation, and the uniqueness of modern sea-level rise[1]. Kench et al.[2] recently reconstructed Common-Era sea level in the Maldives, Indian Ocean, using coral microatolls. They reported periods of 150–500 yr when sea level fell and rose at average rates of 2.7–4.3 mm yr^{-1}. These periods coincided with intervals of cooling and warming inferred from proxy reconstructions of sea-surface temperature (SST) and radiative forcing (ref. 2, Fig. 2). Kench et al.[2] reasoned that these 0.6–1.4-m centennial-scale sea-level fluctuations were driven by climate, specifically thermal contraction and expansion of seawater. In contrast to previous studies[3,4], Kench et al.[2] argued that modern rates and magnitudes of sea-level rise caused by climate change have precedent during the Common Era. We use principles of sea-level physics to argue that pre-industrial radiative forcing and SST changes were insufficient to cause thermosteric sea-level (TSL) trends as large as reported for the Maldives[2].

Radiative forcing (e.g., related to solar activity[5] and volcanic eruptions[6]) varies over a broad range of time scales, and influences global climate and sea level[7,8]. For example, models show that major volcanic eruptions during the twentieth century drove rapid interannual falls in global-mean sea level (order mm yr^{-1}) that were followed by gradual decadal rises (order tenths of mm yr^{-1}) as the climate system recovered[7]. To determine whether variability in radiative forcing on centennial and longer time scales in the Common Era was sufficient to drive TSL trends as large and sustained as those inferred for the Maldives[2], we express trends in TSL in terms of their equivalent net surface heat flux (see Supplementary Information). Using a thermal expansion coefficient characteristic of tropical surface ocean waters (3.1–3.4×10^{-4} $°C^{-1}$), we estimate that a net flux of 1.0–1.8 W m^{-2} is required for a TSL trend of 2.7–4.3 mm yr^{-1}. The required flux is stronger than centennial-scale variations in reconstructions of radiative forcing[5,6], which can be uncertain, but exhibit magnitudes < 0.4 and < 0.2 W m^{-2} over time scales of 150 and 500 yr, respectively (95% confidence; Fig. 1a; Supplementary Information). In other words, radiative forcing likely accounts for $< 31\%$ ($< 18\%$) of the forcing required to produce 150-yr (500-yr) TSL trends of 2.7–4.3 mm yr^{-1} (Fig. 1c, purple). This required net heat flux is also larger than the rate of contemporary global upper-ocean warming since 2005 CE (0.5–0.7 W m^{-2}) estimated from profiling-float observations[9].

We also estimate what SST trend is required to generate a given trend in TSL (Supplementary Information). We assume that magnitudes of ocean temperature changes decay exponentially from the surface to the bottom over an e-folding depth scale of 750–1250 m. This translates to 45–61% (83–94%) of ocean heat storage occurring in the upper 700 m (2000 m), similar to estimates from model-data syntheses[10,11] of changes in global ocean heat content over the past 140–270 yr. Using a reasonable global-ocean, volume-averaged thermal expansion coefficient (1.6–1.9×10^{-4} °C^{-1}), we find that TSL trends of 2.7–4.3 mm yr^{-1} require attendant SST trends of 1.2–3.6 °C century^{-1} (Fig. 1b). This estimate is supported by long integrations of an empirical ocean circulation model[12], which suggest that TSL trends of 2.7–4.3 mm yr^{-1} sustained for 150 and 500 yr require SST trends of 1.8–2.9 and 0.9–1.4 °C century^{-1}, respectively (Fig. 1b; Supplementary Information). These model results are consistent with the basic expectation that, on longer time scales under sustained climate forcing, relatively more heat penetrates the deep ocean, requiring a comparatively smaller SST change to produce a given TSL trend.

The required SST trends are larger than observed in ten reconstructions of Common-Era SST[13] in the Indian Ocean and Indonesian Throughflow, which show trends of < 0.8 and < 0.2 °C century^{-1} on time scales of 150 and 500 yr, respectively (95% confidence; Fig. 1b; Supplementary Information). Although they are not from the Maldives, these SST reconstructions are informative of the range of reconstructed centennial SST trends over the tropical Indian Ocean during the Common Era. We find that SST reconstructions likely account for $< 37\%$ and $< 7\%$ of the temperature trends needed to explain TSL trends of 2.7–4.3 mm yr^{-1} on time scales of 150 and 500 yr, respectively, assuming exponential vertical structure (Fig. 1c, blue). Using the empirical ocean circulation model, we estimate corresponding percentages of $< 33\%$ and $< 13\%$ (Fig. 1c, orange). Even making the extreme assumption that ocean temperature trends are vertically uniform, which is unrealistic given the long adjustment time scales in the deep ocean[12], we find that SST trends required for trends in TSL of 2.7–4.3 mm yr^{-1} (Fig. 1b) are generally larger than are inferred from SST reconstructions, especially for periods > 300 yr (Fig. 1c, green).

Kench et al.[2] reconstructed a sea-level trend of 4.2 mm yr^{-1} in the Maldives for the modern industrial interval between 1807 and 2018 CE. Comparable trends of 3.2–4.7 mm yr^{-1} are seen in two tide-gauge sea-level records[14] in the Maldives for the past 25–30 yr (Supplementary Table S1). However, smaller sea-level trends of 0.6–1.5 mm yr^{-1} are seen for the past 80–140 yr in four long tide-gauge records along the Indian coast (Supplementary Table S1). This underscores that sea-level trends are time-scale dependent, and can be influenced by stochastic processes that tend to decrease in magnitude with increasing time scale (Supplementary Information). Moreover, the Indian tide gauges show good correlation with, and similar trends to, the tide gauges from the Maldives for the overlapping interval since ~ 1990 CE (Fig. 1d; Supplementary Table S1). This means that the tide gauges in India are informative of sea-level variability more broadly across the region through time. Thus, the average rate of sea-level rise since 1807 CE reconstructed by Kench et al.[2] in the Maldives from coral microatolls is faster than the quasi-centennial rates measured by nearby tide gauges, and is too large to be understood in terms of large-scale climate alone.

To address the lack of near-continuous Common-Era sea-level reconstructions in the Indian Ocean, Kench et al.[2] reconstructed sea level in the Maldives over the past two millennia using fossil corals. We suggest that the 0.6–1.4-m centennial sea-level changes in the Maldives are too large to have resulted from the thermal contraction and expansion of seawater related to large-scale climate forcing alone. We quantify how exceptional ocean cooling or warming near the Maldives would have been in a larger context were they sufficient to drive centennial sea-level trends as large as those determined by Kench et al.[2]. As Kench et al.[2] acknowledged, it is also unlikely that these centennial sea-level changes reflect surface ice and water mass redistribution[15], since similar coeval changes are not supported by other intermediate- and far-field Common-Era sea level reconstructions[3,4]. We hypothesize that local-scale processes probably drove the apparent sea-level lowstands in the Maldives. One possibility is that the corals used to reconstruct sea level sustained erosion, which could render them biased (low) recorders of sea level (Supplementary Information). Images of example corals from the Maldives shown by Kench et al.[2] (ref. 2, Supplementary Fig. 3) feature planar surfaces without concentric growth rings, which may indicate erosion. If the corals used for reconstructing sea level in the Maldives were eroded, then sea-level variability, radiative forcing, and ocean physics could be reconciled, suggesting that the records of Kench et al.[2] should not be interpreted as a Common-Era precedent for modern rates of sea-level rise related to climate. More proxy reconstructions from the Maldives and the wider tropical Indian Ocean are necessary to replicate the Maldives sea-level reconstruction, and more comprehensively quantify local, regional, and global changes in sea level during the Common Era.

References

1. Kemp, A. C. et al. Paleo constraints on future sea-level rise. *Curr. Clim. Change Rep.*, **1**, 205–215 (2015).

2. Kench, P. S. et al. Climate-forced sea-level lowstands in the Indian Ocean during the last two millennia. *Nat. Geosci.*, **13**, 61–64 (2020).

3. Kemp, A. C. et al. Climate related sea-level variations over the past two millennia. *P. Natl. Acad. Sci. U.S.A.*, **108**(27), 11017–11022 (2011).

4. Kopp, R. E. et al. Temperature-driven global sea-level variability in the Common Era. *P. Natl. Acad. Sci. U.S.A.*, **113**(11), E1434–E1441 (2016).

5. Steinhilber, F. et al. Total solar irradiance during the Holocene. *Geophys. Res. Lett.*, **36**, L19704 (2009).

6. Sigl, M. et al. Timing and climate forcing of volcanic eruptions for the past 2,500 years. *Nature*, **523**, 543–549 (2015).

7. Church, J. A. et al. Significant decadal-scale impact of volcanic eruptions on sea level and ocean heat content. *Nature*, **438**, 74–77 (2005).

8. Gleckler, P. J. et al. Krakatoa lives: The effect of volcanic eruptions on ocean heat content and thermal expansion. *Geophys. Res. Lett.*, **33**, L17702 (2006).

9. Cheng, L. et al. How fast are the oceans warming? *Science*, **363**, 128–129 (2019).

10. Zanna, L., et al. Global reconstruction of historical ocean heat storage and transport. *P. Natl. Acad. Sci. U.S.A.*, **116**(4), 1126–1131 (2019).

11. Gebbie, G., & Huybers, P. The Little Ice Age and 20th-century deep Pacific cooling. *Science*, **363**, 70–74 (2019).

12. Gebbie, G., & Huybers, P. The mean age of ocean waters inferred from radiocarbon observations: sensitivity to surface sources and accounting for mixing histories. *J. Phys. Oceanogr.*, **42**, 291–305 (2012).

13. Emile-Geay, J. et al. A global multiproxy database for temperature reconstructions of the Common Era. *Sci. Data*, **4**, 170088 (2017).

14. Holgate, S. J. et al. New data systems and products at the permanent service for mean sea level. *J. Coastal Res.*, **29**(3), 493–504 (2013).

15. Tamisiea, M. E., & Mitrovica, J. X. The moving boundaries of sea level change: understanding the origins of geographic variability. *Oceanography*, **24**(2), 24–39 (2011).

Supplementary Information is linked to the online version of the paper at www.nature.com/ngeo.

Acknowledgments CGP acknowledges support from NSF grant OCE-2002485, The Andrew W. Mellon Foundation Endowed Fund for Innovative Research and The Joint Initiative Awards Fund from the Andrew W. Mellon Foundation at the Woods Hole Oceanographic Institution. GG acknowledges support from NSF grant OCE-1760958. AM acknowledges support from the National Research Foundation Singapore and the Singapore Ministry of Education under the Research Centres of Excellence initiative, and also from the National Research Foundation Singapore under its NRF Fellowship scheme (Award NRF-NRFF11-2019-0008). We thank Paul Kench for helpful conversations on an earlier version of the manuscript.

Author Contributions CGP, ACK, and GG conceived of the study. All of the authors designed methods and analyzed data. CGP wrote the manuscript with input from ACK, GG, and AJM.

Competing Interests The authors declare that they have no competing financial interests.

Correspondence Correspondence and requests should be addressed to CGP (cpiecuch@whoi.edu).

Data Availability Temperature-sensitive Common-Era proxy records from the PAGES2k project[13] were taken from the current data version available from the National Climatic Data Center website on 22 Jan 2020 (`www1.ncdc.noaa.gov/pub/data/paleo/pages2k/pages2k-temperature-v2-2017/`). Only low-resolution oceanic data ("O2kLR") covering most of the Common Era in the study area were used. Numerical codes for the circulation model from Gebbie and Huybers[12] are available for download from GG's website (`https://www2.whoi.edu/staff/ggebbie/`). Total solar irradiance during the Holocene from Steinhilber et al.[5] was downloaded from the National Climatic Data Center FTP server on 3 Feb 2020 (`ftp.ncdc.noaa.gov/pub/data/paleo/climate_forcing/solar_variability/`). The estimates of volcanic aerosol forcing from Sigl et al.[6] are as provided in the online version of the paper as of 3 Feb 2020 (`https://www.nature.com/articles/nature14565`). The tide-gauge sea-level data were extracted from the Permanent Service for Mean Sea Level (PSMSL) database[14] on 24 Feb 2020 (`https://www.psmsl.org/data/obtaining/`).

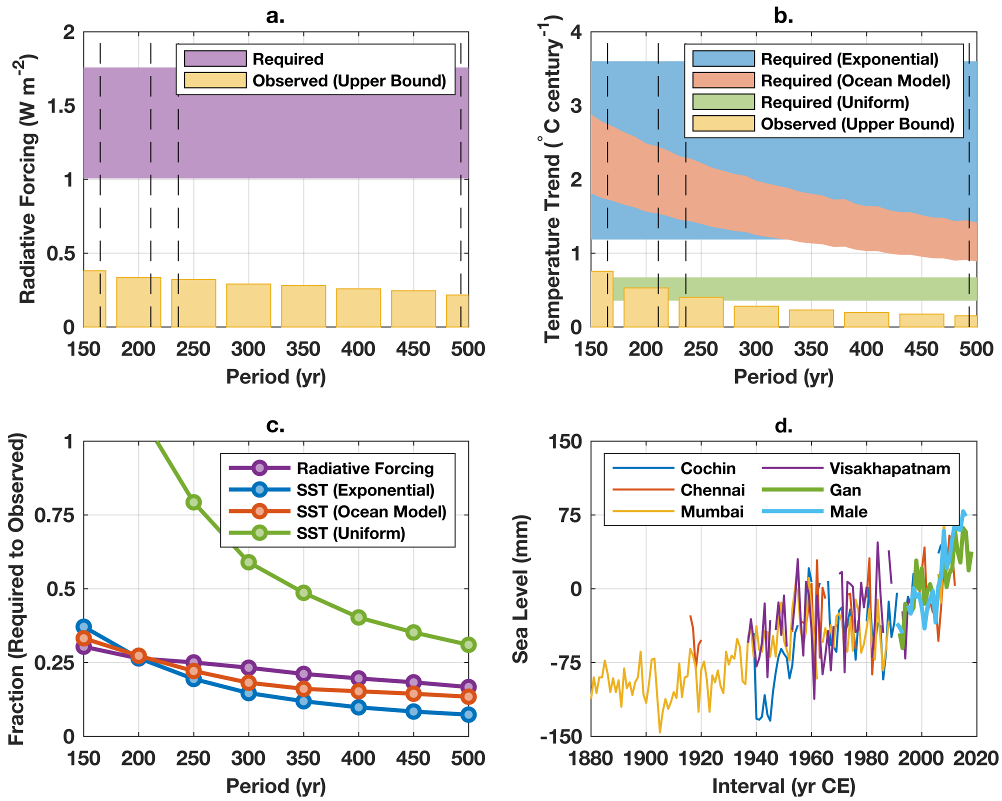

Figure 1. a, Net surface heat flux required to generate a trend in thermosteric sea level (TSL) of 2.7–4.3 mm yr^{-1} (purple shading) exceeds the radiative-forcing magnitudes that likely took place during 0–1800 CE on time scales of 150–500 yr (yellow bars; see Supplementary Information). Dashed vertical black lines indicate the duration of sea-level trends reconstructed by Kench et al.[2] for the Maldives (corresponding to -91 to 401, 552 to 717, 1521 to 1757, and 1807 to 2018 CE). **b,** Sea-surface-temperature (SST) trends needed to generate a trend in TSL of 2.7–4.3 mm yr^{-1} for 150–500 yr based on the assumption that ocean temperature trends decay exponentially with ocean depth (blue shading) and from an empirical ocean circulation model[12] (orange shading) exceed the SST trends that likely took place during 0–1800 CE on time scales of 150–500 yr (yellow bars;

see Supplementary Information). Only in the unrealistic case of assumed vertically uniform ocean heat storage do the SST trends needed for TSL trends of 2.7–4.3 mm yr^{-1} (green shading) overlap with the likely proxy-observed values, and then only for periods < 300 yr. Dashed vertical black lines are as in **a**. **c,** Radiative-forcing magnitudes and SST trends that took place over 0–1800 CE on time scales of 150–500 yr likely represent only a fraction (vertical axis) of the changes needed to produce TSL trends of 2.7–4.3 mm yr^{-1} (Supplementary Information). **d,** Tide-gauge sea-level records[14] from India (Cochin, Chennai, Mumbai, Visakhapatnam) are correlated with data records from the Maldives (Gan, Male) for the overlapping interval since ~ 1990. The records from India show longterm trends of 0.6–1.5 mm yr^{-1}, which is smaller than the value of 4.2 mm yr^{-1} reported by Kench et al.[2] for the Maldives between 1807–2018 CE using coral microatolls. Tide-gauge time series are centered on their average value during 1990–2013 CE.

Supplementary Information

Calculation of equivalent surface heat flux Heat conservation and hydrostatic balance together dictate that a net surface heat flux Q effects a change in thermosteric sea level (TSL) h_T following,

$$\dot{h_T} = \frac{\alpha}{c_p \rho_0} Q, \tag{1}$$

where dot is time derivative, α thermal expansion coefficient, c_p specific heat capacity of seawater, and ρ_0 density of seawater. Rearranging to solve for Q gives,

$$Q = \frac{c_p \rho_0}{\alpha} \dot{h_T}. \tag{2}$$

Values of 1.0–1.8 W m^{-2} quoted in the main text and shown in Fig. 1a are minimum and maximum values computed from Eq. (2) using $\dot{h_T} \in \{2.7, 4.3\}$ mm yr^{-1} and $\alpha \in \{3.1, 3.4\} \times 10^{-4}$ °C^{-1}. We use representative values of $c_p = 4 \times 10^3$ J kg^{-1} °C^{-1} and $\rho_0 = 1 \times 10^3$ kg m^{-3}.

Note that this formulation is in terms of a *net* heat flux Q, and does not explicitly account for any damping effects[16]. As such, Q values computed here should be interpreted as the *minimum* radiative-forcing anomaly needed to generate a given TSL trend. In other words, ratios of observed to required radiative forcing (purple curve in Fig. 1c; see below) are conservative in the sense that they represent upper bounds.

Calculation of centennial anomalies in radiative forcing based on proxies To estimate radiative forcing, we summed together the 40-yr running-mean total solar irradiance values from Steinhilber et al.[5] (linearly interpolated onto a yearly spacing) and annual atmospheric aerosol loading owing to volcanic eruptions determined by Sigl et al.[6] (zero values were imputed for years without volcanic eruptions) and removed the time average over the interval 0–1800 CE (Supplementary Fig. S1a–c). We computed running averages of the reconstructed radiative-forcing anomaly series for averaging periods between 150 and 500 yr in 50-yr increments (Supplementary Fig. S1d). With each of these running-average time series, we computed absolute values and evaluated the 95th percentile of the resulting time-smoothed radiative-forcing anomaly magnitude record (Supplementary Fig. S1e–f). These 95th percentiles (yellow bars in Fig. 1a) reflect upper bounds on the radiative forcing values at a given time scale (i.e., 95% of values are smaller than this). Implicit in our analysis, following ref. 2, is the assumption that this global forcing applies over the central equatorial Indian Ocean.

To quantify, in a relative sense, to what extent the reconstructed radiative-forcing anomalies were sufficient to generate TSL trends as large as the trends inferred in the Maldives[2], we evaluated the ratio of the reconstructed radiative-forcing anomaly as a function of time scale (Supplementary Fig. S1e–f) to the required radiative forcing estimated using Equation 2 (purple shading in Fig. 1a, assumed to be a uniform distribution) and took 95th percentiles, giving the purple values shown in Fig. 1c (cf. discussion below related to a similar calculation for SST trends).

Calculation of the implied sea-surface-temperature (SST) trend Trends in TSL $\dot{h_T}$ are related to ocean temperature trends $\dot{T}(z)$ according to,

$$\dot{h_T} = \int_{-H}^{0} \alpha \, \dot{T}(z) \, dz, \tag{3}$$

where z is the vertical coordinate (positive upwards) and H the ocean depth. In the scaling analysis, we assumed that,

$$\dot{T}(z) = \dot{T}_0 \exp\left(z/H_T\right). \tag{4}$$

Integrating and rearranging, we obtain the analytical solution for $\dot{T}_0$, which is the SST trend,

$$\dot{T}_0 = \frac{\dot{h_T}}{\alpha H_T} \left[1 - \exp\left(-H/H_T\right)\right]^{-1}. \tag{5}$$

Values of 1.2–3.6 °C century^{-1} in the main text are the minimum and maximum values computed from Eq. (5) using $\dot{h_T} \in \{2.7, 4.3\}$ mm yr^{-1}, $\alpha \in \{1.6, 1.9\} \times 10^{-4}$ °C^{-1}, $H_T \in \{750, 1250\}$ m, and $H = 4 \times 10^3$ m (cf. blue shading in Fig. 1b).

Assuming instead that $\dot{T}$ is vertically uniform, Eq. (5) reduces to the simplified form,

$$\dot{T}_0 = \frac{\dot{h_T}}{\alpha H} \tag{6}$$

Evaluating this equation using the same parameter values, and taking the minimum and maximum, we obtain the green shading in Fig. 1b.

Choice of e-folding depth scale We chose a range of 750–1250 m for the e-folding scale H_T of ocean temperature changes. This choice was motivated by published estimates[10,11] of global-ocean heat storage during the past 140–270 yr. The reconstruction of Zanna et al.[10] suggests that $\sim 75\%$ of global ocean heat storage since 1871 occurred in the upper 700 m and $\sim 95\%$ in the top 2000 m (their Fig. 1a–1c). The model simulation of Gebbie and Huybers[11] calculated from equilibrium at 1750 CE shows that $\sim 50\%$ and $\sim 85\%$ of the ocean heat content changes occurred at depths above 700 and 2000 m, respectively (their Fig. 4b). Since the 140–270-yr time scales highlighted in these studies[10,11] are on the short end of the 150–500-yr range considered here[2], we selected 750–1250 m for the e-folding depth scale as conservative values that allow comparatively more heat to penetrate the deep ocean, requiring a smaller change in SST to achieve a given TSL trend.

Circulation model calculations We run the circulation model from Gebbie and Huybers[12] with idealized concentration (Dirichlet) boundary conditions. We perform 100 iterations of a $40,000$-yr simulation with randomized phasing of the boundary conditions. Surface boundary conditions are globally uniform and follow a frequency spectrum with a power law of -1.64 following Huybers and Curry[17]. We use the global Green's function (or transit-time distribution) to produce simulated time series, and results are similar if we use four surface patches to account for climate hemispheric asymmetries. We consider non-overlapping intervals of between 150 and 500 yr (10-yr increments) and compute SST and TSL trends within the equatorial Indian Ocean near the Maldives ($4°$N $78°$E; 3750-m depth). For each trend window, we fit a first-order least-squares trend line to all TSL-SST trend pairs (Supplementary Fig. S2). The slope of this fit was taken to be the SST change per unit change in TSL for a particular time scale. For example, we found that a trend of 1 mm yr^{-1} in TSL corresponds to a SST trend of 0.67 and 0.33 $°$C century^{-1} at respective time scales of 150 and 500 yr. Slopes are multiplied by 2.7–4.3 mm yr^{-1} to produce the orange-shaded region in Fig. 1b.

Calculation of centennial SST trends from temperature-sensitive proxy data We analyzed all Common-Era SST proxy reconstructions from the PAGES2k consortium[13] from the Indian Ocean and around the Indonesian Throughflow (see Data Availability). This data set comprises one record each from the Arabian Sea, Horn of Africa, southwest coast of India, the Philippines, South China Sea, and western equatorial Pacific, and four in Makassar Strait (Supplementary Figs. S3, S4a–j). We linearly interpolated each available record onto a common yearly interval, and then computed trends from each record for every 150- to 500-yr period between 0–1800 CE. This procedure gave a separate time series with all possible trends across the ten proxy locations for each trend period between 150 and 500 yr. With each period-specific trend time series, we removed the overall mean, took absolute values, and then computed the 95th percentile of these anomalous trend magnitudes (Supplementary Fig. S4k–l). These 95th percentiles (yellow bars in Fig. 1b) reflect upper bounds on the proxy SST trends at a given time scale (i.e., 95% of trends are smaller than these values).

Note that these SST proxies are not from the Maldives and thus are not truly collocated with the sea-level reconstruction from Kench et al.[2]. Our approach follows that of Kench et al.[2] in that we use available SST proxy records from nearby locations to interpret the sea-level reconstruction from the Maldives, where "nearby" is taken to mean "in the Indian Ocean or around the Indonesian Throughflow." However, we consider more SST records than do Kench et al.[2], including a record from the southwest coast of India, which is $< 1,000$ km from the sea-level reconstruction in the Maldives (Supplementary Fig. S3). Our calculations should thus be interpreted as spanning a plausible envelope of possible SST trends (as a function of time scale) across the tropical Indian Ocean during the Common Era. We believe that the true Common-Era SST history in the Maldives is within this realistic range. In other words, our results quantify how unusual the SST trends in the Maldives would have been, within a larger regional context, to be large enough to drive the sea-level trends inferred by Kench et al.[2].

As with radiative forcing, we quantified the relative extent to which reconstructed SST trends were large enough to generate TSL trends as large as those in the sea-level reconstruction from the Maldives[2]. We evaluated the ratio of the amplitudes of reconstructed SST trends (Supplementary Fig. S4k–l) to the required SST trends using Equations 5 and 6 and from the empirical circulation model[12] (blue, green, and orange shading in Fig. 1b, respectively, which we assumed were uniform distributions) and took the 95th percentiles as a function of time scale. This method produced the respective blue, green, and orange values in Fig. 1c.

Instrumental tide-gauge sea-level data To interpret the most recent (1807–2018 CE) sea-level trend for the Maldives from Kench et al.[2], we used tide-gauge annual-mean sea-level records from the Permanent Service for Mean Sea Level[14] (see Data Availability). We used all > 70-yr records in the database from along coastal India (four time series) and from the Maldives (two time series). For all records, we computed best estimates of least-squares trends to the available data, ignoring data gaps. The trend values are given in Supplementary Table S1. Note that we did not consider the long (82-yr) tide-gauge record from Garden Reach, India, since it is located far upstream in the Bhāgirathi-Hooghly, near Kolkata, and is not reflective of large-scale, open-ocean conditions.

The sea-level trends from tide-gauge data quoted in the main text (Supplementary Table S1) were computed over the full record lengths of the respective time series. To quantify the sensitivity of the trends to time scale, we computed trends in the tide-gauge data for all possible time intervals ≥ 20 yr using the longest and most continuous records from Visakhapatnam, Mumbai, and Cochin (Supplementary Fig. S5). While larger trends are possible and observed in the tide-gauge data over shorter periods (e.g., trends of 4–7 mm yr^{-1} over periods of 20–30 yr), trends over longer intervals have smaller amplitudes (e.g., $\lesssim 3$ mm yr^{-1} for $\gtrsim 40$-yr periods). Trends as large and sustained as those reported by Kench et al.[2] in the Maldives during 1807–2018 CE (~ 4 mm yr^{-1}) are therefore not supported by a more general, in-depth analysis of the tide-gauge data.

Interpretation of corals A microatoll is a coral colony with a living outer margin, but with a dead upper surface. Microatolls typically form concentric rings on their upper surfaces related to interannual variability in lowest water levels and highest levels of survival[26]. A microatoll growing during decadal periods of stable sea level will record little net elevation change from its center to its outer perimeter, even as concentric rings grow up and die down over shorter periods. If sea level rises or falls during the lifetime of a microatoll, its outer perimeter will be higher or lower, respectively, than its center. After a microatoll dies, this concentric ring morphology remains recognizable unless the coral's upper surface experiences substantial erosion (e.g., ref. 27, Fig. 6). Corals that remain in the intertidal zone for extended periods of time after death can sustain intense bioerosion[28].

Most of the fossil corals in the photographs from Mahutigalaa (ref. 2, Supplementary Fig. 3) exhibit flat upper surfaces. They show no clear elevation changes from their centers to their outer perimeters. If these corals are uneroded, then this morphology indicates that sea levels were stable during coral growth. However, if there was rapid sea-level change during the lifetimes of the corals, some of them would be expected to show much higher or lower outer perimeters compared to their centers. If each coral is flat and uneroded but has a different elevation, it would imply that sea level was stable over long periods as each coral grew, with punctuated sea-level changes limited to short intervals from which no microatolls are preserved. Alternatively, the flat tops of the corals could plausibly be explained by erosion, such that each coral was planed off at a level below its original height of living coral. In that case, the coral would reflect a limiting (minimum) data point, and the true sea level could have been higher.

In addition to the lack of net elevation gain or loss exhibited by any of the Mahutigalaa corals, most of the corals look to have smooth, planar surfaces, and there is no clear evidence of concentric rings. This also suggests erosion of the corals. For groups of roughly coeval corals in their data set, Kench et al.[2] discarded the higher corals as outliers, suggesting that their higher elevations resulted from ponding. Instead, we propose that the lower corals from each group may have been more eroded. Kench et al.[2] based their reconstruction on the lower, possibly planed-off corals. But, if the higher fossil corals provide the best estimate of sea level in the Maldives at any particular time, then sea level during the lowstands reported by Kench et al.[2] may never have fallen lower than 0.4–0.5 m below current sea level in 2018 CE.

Additional References

16. Douglass, D. H. & Knox, R. S. Climate forcing by the volcanic eruption of Mount Pinatubo. *Geophys. Res. Lett.*, **32**, L05710 (2005).

17. Huybers, P. & Curry, W. Links between annual, Milankovitch and continuum temperature variability. *Nature*, **441**, 329–332 (2006).

18. Tierney, J. E. et al. Past and future rainfall in the Horn of Africa. *Sci. Adv.*, **1**(9), e1500682 (2015).

19. Doose-Rolinski, H. et al. High-resolution temperature and evaporation changes during the Late Holocene in the northeastern Arabian Sea. *Paleoceanography*, **16**(4), 358–367 (2001).

20. Saraswat, R. et al. Deglaciation in the tropical Indian Ocean driven by interplay between the regional monsoon and global teleconnection. *Earth Planet. Sc. Lett.*, **375**, 166–175 (2013).

21. Zhao, M. et al. A millennial-scale $U_{37}^{K'}$ sea-surface temperature record from the South China Sea (8°N) over the last 150 kyr: Monsoon and sea-level influence. *Palaeogeogr. Palaeocl.*, **236**(1–2), 39–55 (2006).

22. Linsley, B. K. et al. Holocene evolution of the Indonesian throughflow and the western Pacific warm pool. *Nat. Geosci.*, **3**, 578–583 (2010).

23. Newton, A. et al. Changes in the Indonesian Throughflow during the past 2000 yr. *Geology*, **39**(1), 63–66 (2011).

24. Oppo, D. W. et al. 2,000-year-long temperature and hydrology reconstructions from the Indo-Pacific warm pool. *Nature*, **460**, 1113–1116 (2009).

25. Stott, L. et al. Southern Hemisphere and Deep-Sea Warming Led Deglacial Atmospheric CO_2 Rise and Tropical Warming. *Science*, **318**(5849), 435–438 (2007).

26. Meltzner, A. J., & Woodroffe, C. D. Coral microatolls, in *Handbook of Sea-Level Research*, Shennan, I. et al. (Editors), John Wiley & Sons, Chichester, UK, pp. 125–145 (2015).

27. Majewski, J. M. et al. Holocene relative sea-level records from coral microatolls in Western Borneo, South China Sea. *The Holocene*, **28**(9), 1431–1442 (2018).

28. Taylor, F. W. et al. Analysis of partially emerged corals and reef terraces in the central Vanuatu Arc: Comparison of contemporary coseismic and nonseismic with Quaternary vertical movements. *J. Geophys. Res.*, **92**, 4905–4933 (1987).

Location	Lat (°N)	Lon (°E)	Trend (mm yr^{-1})	Length (yr)
Chennai, India	13	80	0.57 (1.87)	1916–2015
Visakhapatnam, India	18	83	0.92 (3.95)	1937–2013
Mumbai, India	19	73	0.84 (4.21)	1878–2015
Cochin, India	10	76	1.51 (3.23)	1939–2013
Gan, Maldives	−1	73	3.21	1989–2018
Male, Maldives	4	74	4.70	1991–2016

Supplementary Table S1. Names, locations, and record lengths of tide-gauge sea-level records used here. The trend is the best estimate of the slope of a least-squares linear fit to the available data (ignoring any data gaps). Parenthetical values for Indian tide gauges (Chennai, Visakhapatnam, Mumbai, Cochin) are trends since 1990 for direct comparison with the trends from the Maldivian gauges (Gan, Male).

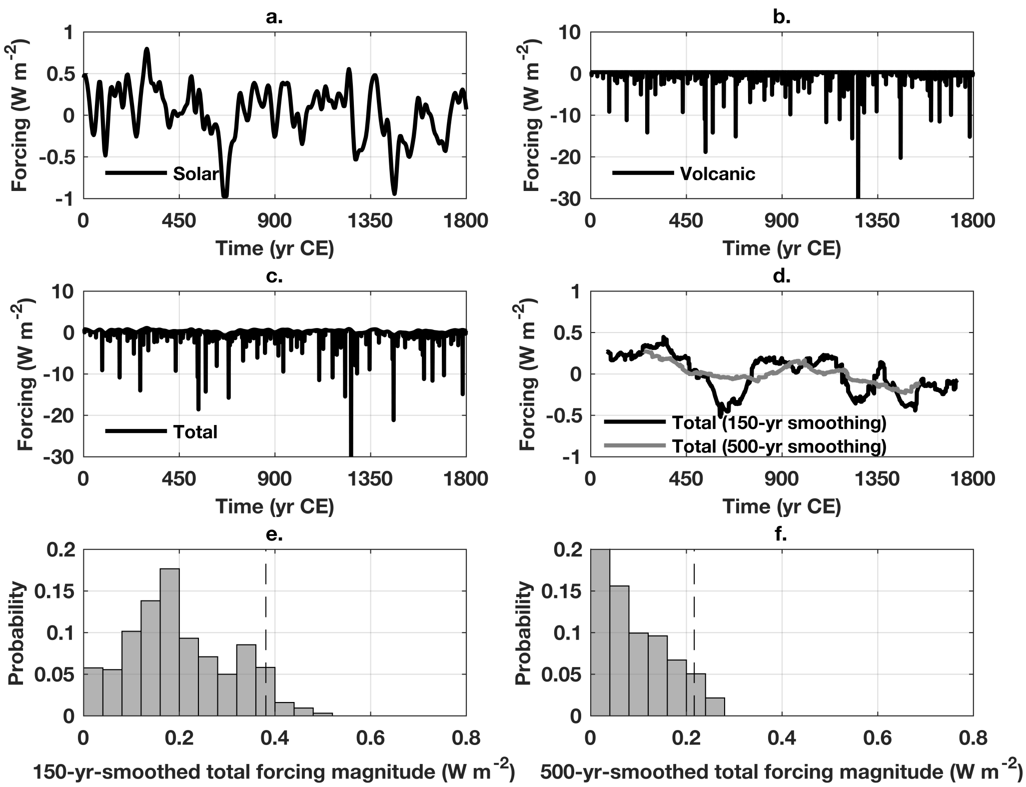

Supplementary Figure S1. a, Solar irradiance from Steinhilber et al.[5]. **b,** Volcanic aerosol forcing from Sigl et al.[6]. **c,** Total radiative forcing (sum of time series from panels **a** and **b**). **d,** Smoothed radiative forcing (time series from panel **c** with a 150- and 500-yr running-mean smoother applied). Mean values during 0–1800 CE are removed from the time series in panels **a–d**. **e,** Histogram of 150-yr-smoothed forcing amplitudes from panel **d**. Black dashed vertical line is the 95th percentile. **f,** As in **e** but for 500-yr-smoothed values.

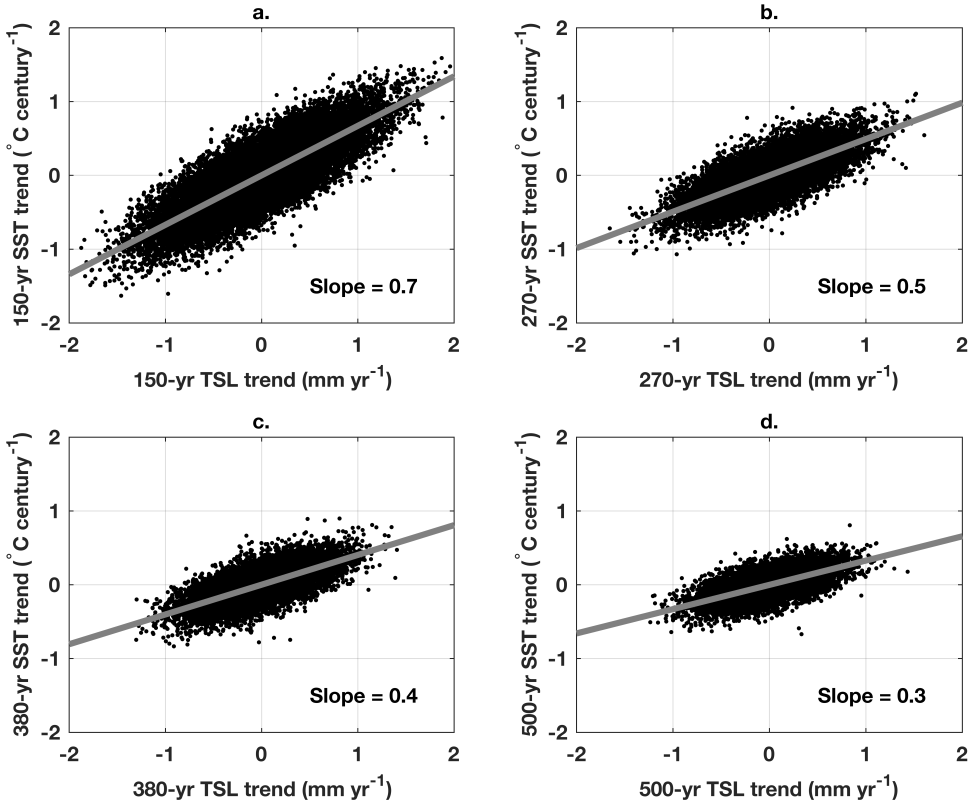

Supplementary Figure S2. **a,** Black dots are all pairs of 150-yr TSL and SST trends from the long empirical circulation model integrations. Gray line is a trend line fit to the scatter, where the slope (indicated to the bottom right) is the change in SST trend per unit change in TSL trend in units of $(^\circ\mathrm{C\ century}^{-1})/(\mathrm{mm\ yr}^{-1})$. **b–d,** As in **a** but for periods of **b,** 270 yr, **c,** 380 yr, and **d,** 500 yr. Longer periods permit a more vertically homogeneous temperature response.

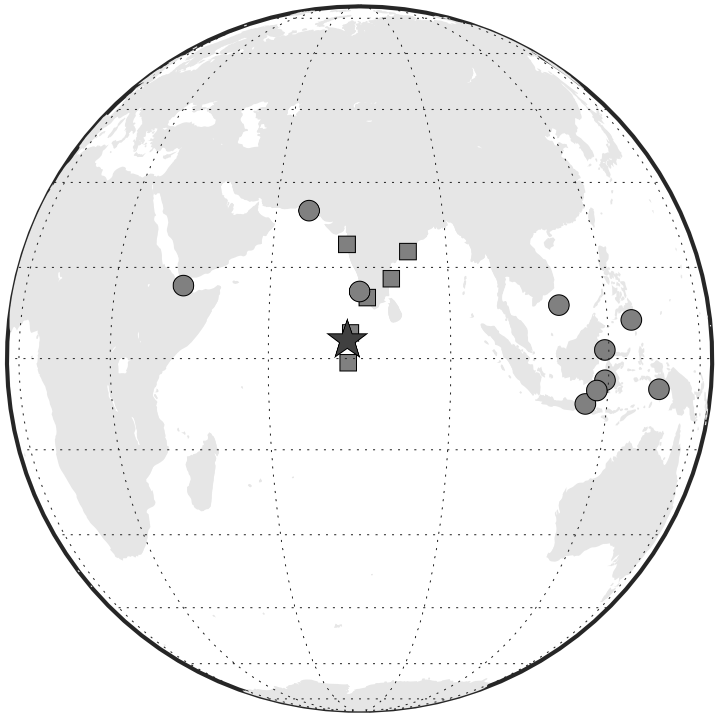

Supplementary Figure S3. Locations of proxy and instrumental data assets used in this study. Dark gray star is the location of the sea-level reconstruction from the Maldives. Light gray circles and squares are, respectively, are the locations of SST proxies and tide-gauge sea-level records.

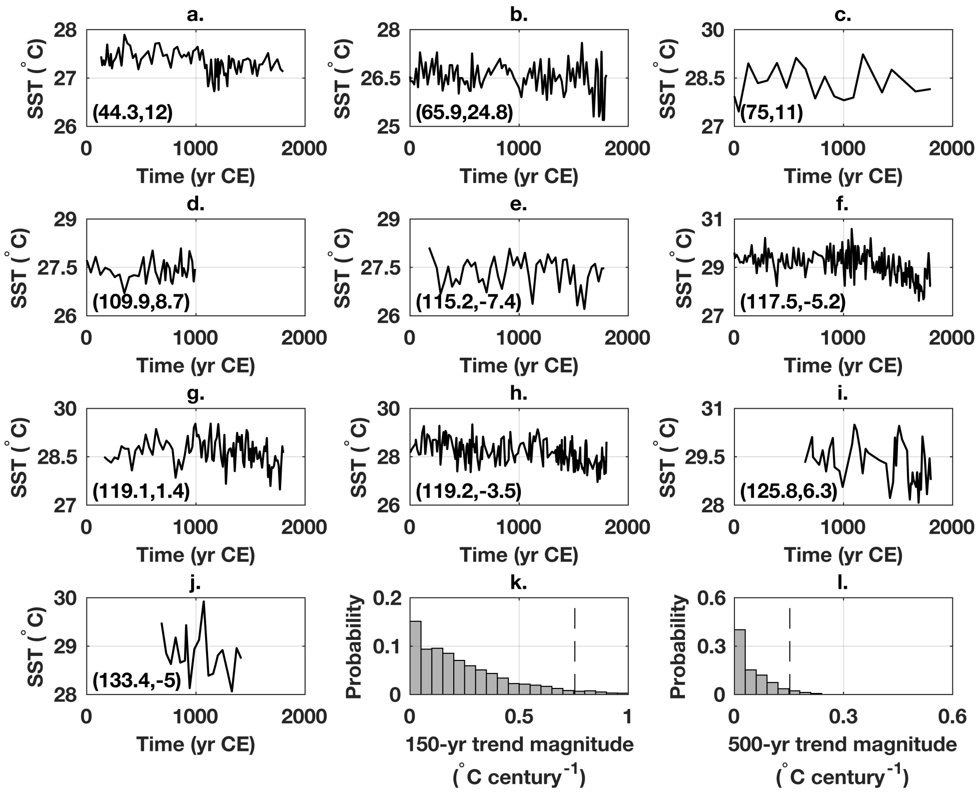

Supplementary Figure S4. Common-Era proxy SST reconstructions from **a,** Horn of Africa[18], **b,** Arabian Sea[19], **c,** southwest coast of India[20], **d,** South China Sea[21], **e–h,** Makassar Strait[22–24], **i,** Philippines[25], and **j,** western equatorial Pacific[25]. Longitude (°E) and latitude (°N) are given in parenthesis at bottom left. Histograms of anomalous SST trend amplitudes across all ten sites for **k,** 150-yr and **l,** 500-yr periods. Black dashed vertical lines are 95th percentiles of the distributions.

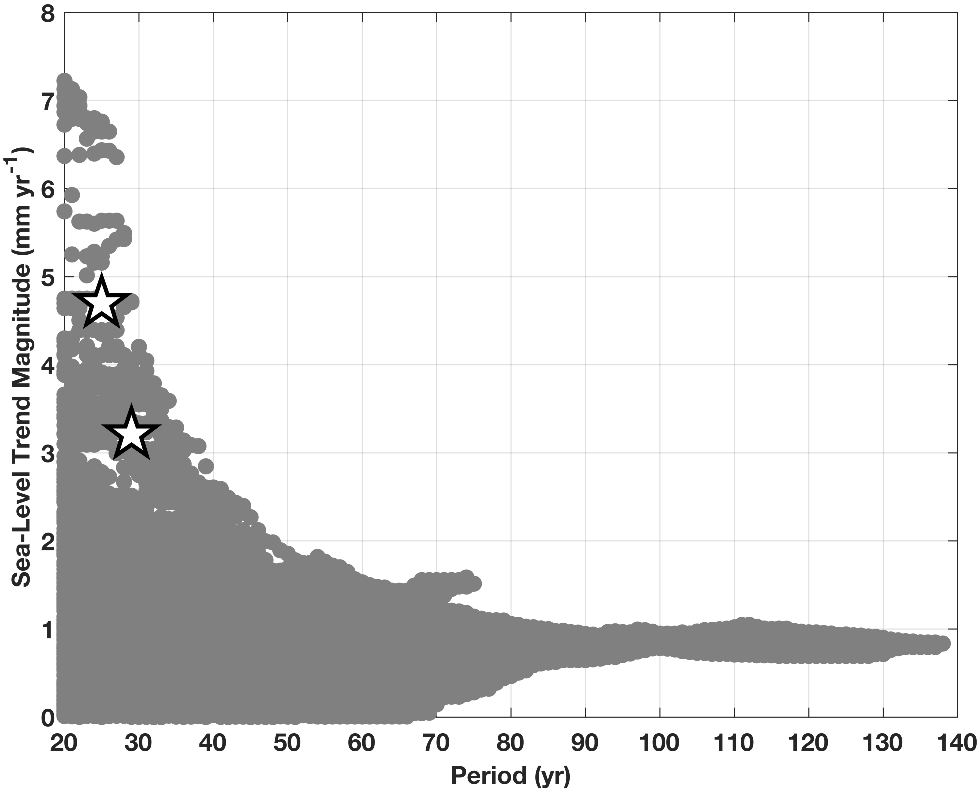

Supplementary Figure S5. Relative sea-level trends computed over all possible time periods from the longer Indian tide-gauge records at Visakhapatnam, Mumbai, and Cochin, shown as a function of period. Stars indicate sea-level trends computed from the shorter Maldivian tide-gauge records at Gan and Male (cf. Supplementary Table S1).